

복합재료에 의한 열전변환 냉각소자의 개발에 관한 연구

논문

9-1-10

Experimental Fabrication and Analysis of Thermoelectric Devices

성만영*, 송대식*, 배원일*

(Man-Young Sung · Dae-Sik Song · Won-Il Bae)

Abstract

This paper has presented the characteristics of thermoelectric devices and the plots of thermoelectric cooling and heating as a function of currents for different temperatures. The maximum cooling and heating (ΔT) for $(\text{BiSb})_2\text{Te}_3$ and $\text{Bi}_2(\text{TeSe})_3$ as a function of currents is about 75°C .

A solderable ceramic insulated thermoelectric module. Each module contains 31 thermoelectric devices. Thermoelectric material is a quaternary alloy of bismuth, tellurium, selenium, and antimony with small amounts of suitable dopants, carefully processed to produce an oriented polycrystalline ingot with superior anisotropic thermoelectric properties. Metallized ceramic plates afford maximum electrical insulation and thermal conduction. Operating temperature range is from -156°C to $+104^\circ\text{C}$. The amount of Peltier cooling is directly proportional to the current through the sample, and the temperature gradient at the thermoelectric materials junctions will depend on the system geometry.

Key Word(중요용어) : Peltier effect(펠티에 효과), Thermoelectric refrigerator(열전변환 냉각소자), Bi-Te-Se Thermoelectric device(Bi-Te-Se 열전변환 소자), Thermoelectric effect(열전변환 효과), Seebeck effect(제벡 효과), Thomson effect(톰슨 효과)

1. INTRODUCTION

A thermoelectric device is a solid state device which has no moving parts, and utilizes heat absorption by Peltier effect at a junction of a thermoelectric materials and a metallic electrode. Its features are small size, low weight, accurate temperature control, and maintenance free operation. In particular, the low noise character of the thermoelectric refrigerator is very suitable for cooling of electric and optoelectric devices.⁽¹⁾⁽²⁾⁽³⁾

Since Joule heat is generated internally in

thermoelectric materials and heat is conducted from the hot junction to the cold junction through the materials, effective heat absorption is reduced. Therefore, a pair of n-type and p-type thermoelectric materials must have a large figure of merit. The figure of merit determines the usefulness of any material in thermoelectric applications. The bismuth-antimony alloys were considered to be the best materials for thermoelectric refrigeration and power generation when the properties of semiconductors such as bismuth telluride were investigated. These semiconductors and their alloys have the highest figure of merit near room temperature and above.⁽⁴⁾

In this paper, the purpose of our study is to investigate the thermoelectric devices usable for cooling systems.

* : 고려대학교 전기공학과
접수일자 : 1995년 8월 8일
심사완료 : 1995년 10월 10일

2. ANALYSIS ON THE TEMPERATURE DISTRIBUTION AND THE ENERGY BALANCE AT THE THERMOELECTRIC MATERIALS JUNCTIONS

The basic diagram for the measurement of thermal conductivity is shown in Fig. 1. The arrangement consists of a source of current, metal contact wires, and the sample. With direct current in the circuit, three principle phenomena will occur. These are the Peltier effect, Joule heating, and thermal conduction.⁽⁵⁾ At room temperature and above, the radiative transfer of heat may become appreciable. If the thermoelectric power and thermal conductivity are rapidly varying functions of temperature, two additional terms in the total energy transport equation will become appreciable. Originally there is no temperature gradient across the specimen, but at the initiation of current, a temperature gradient is developed along the sample by the thermoelectric process. In this section, a relation will be derived connecting the measurable parameters (the thermoelectric power, temperature, and specimen dimensions) with the thermal conductivity of a sample.

As mentioned previously, the temperature gradient in the sample is furnished by the thermoelectric effects at the junctions. A current, I , will be considered to be passing in the direction of increasing z in a p-type sample, carrying heat from the cold junction ($z = -\frac{l}{2}$) at temperature T_c to the hot junction ($z = \frac{l}{2}$) at temperature T_h , where

$T_h > T_c$ as shown in Fig. 1. At the wall, the contact lead wires are maintained at the ambient temperature T_a of the walls of the vessel in which a vacuum is maintained to prevent convection effects. The formal solution of the problem is twofold. In the first part, the temperature distribution in a homogeneous sample satisfying appropriate boundary conditions is derived. In the second, the energy

balance at each junction ($z = \pm \frac{l}{2}$) is obtained, and the resulting equations combined to obtain the desired relation between the thermoelectric parameters.

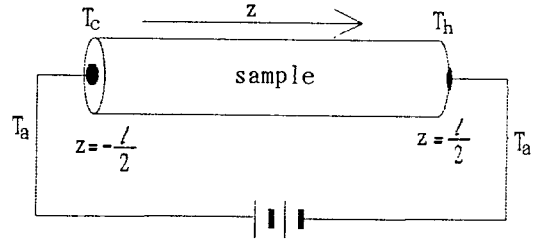


Fig. 1 Experimental arrangement determining thermal conductivity of sample

1) Temperature Distribution⁽⁵⁾

The equation determining the temperature is simply the continuity equation for the total energy flux, which in the steady state is

$$\nabla \cdot \mathbf{U} = 0 \quad (1)$$

From considerations of irreversible thermodynamics, \mathbf{U} is given for isotropic materials by

$$\mathbf{U} = (\alpha T + A) \mathbf{J} - k \nabla T \quad (2)$$

where α is the thermoelectric power, \mathbf{J} is the current density, and k is the thermal conductivity. The gradient of the electrochemical potential, A is given by

$$\nabla A = -\mathbf{J} \rho - \alpha \nabla T \quad (3)$$

where ρ is the electrical resistivity. Substituting Eqs. (2) and (3) in Eq. (1) yields

$$\mathbf{J}^2 \rho - T \mathbf{J} \cdot \nabla \alpha = \nabla \cdot (-k \nabla T) \quad (4)$$

where the charge concentration is assumed stationary so that $\nabla \cdot \mathbf{J} = 0$. For homogeneous materials,

$$\mathbf{J}^2 \rho - \mu_T \mathbf{J} \cdot \nabla T + k \nabla^2 T + (dk/dT)(\nabla T)^2 = 0 \quad (5)$$

where μ_T is the Thomson coefficient, $T \frac{d\alpha}{dT}$. Under the condition that the gradients

of α , k , and ρ are small, Eq. (5) reduces to

$$\nabla^2 T = -\mathbf{J}^2 \rho / k \quad (6)$$

the heat equation with uniform Joule heating in the sample. If the sample has a very small

temperature gradient imposed on it, then it is likely that Eq. (6) will be a good approximation of Eq. (4). Further, for this case, it will be reasonable to assume ρ independent of temperature. It should be kept in mind that the assumptions involved in obtaining Eq. (6) from Eq. (4) may always be examined in the light of subsequent experimental data.

We next consider the boundary conditions. It is assumed that the lead wires have sufficiently small cross section so that radiation from them may be neglected. In the sample, the cross section is considerably larger so that radiation becomes importance. As has been mentioned, in order to obtain a solution of the heat equation, it is necessary to approximate the expression $\sigma \varepsilon (T^4 - T_a^4)$ for the radiation flux by

$4 \sigma \varepsilon \bar{T}^3 (T - T_a)$, where σ is the Stefan-Boltzmann constant, ε is the surface emissivity, and $\bar{T} = (T_h + T_c)/2$. This is a restriction on both T and T_a not to deviate from \bar{T} by more than one third of 1%. The boundary conditions on the ends of the sample are that they should be isothermal. This condition is probably well met since the ends of the sample are covered with a relatively high thermal conductivity solder. A further assumption is made, that even though the diameters of lead wires and sample are quite different, the energy flux in the neighborhood of the junction is parallel to the cylindrical axis. In the case of the lead wires, radiation and axial thermal gradient are neglected. For this case, the total energy flux in the wire is constant, and the temperatures at the ends of the wires are the boundary conditions. In the sample, the particular problem to be solved is the determination of the temperature distribution in right circular cylinder of length l , and radius a , with the following boundary conditions :

$$T(r, -\frac{l}{2}) = T_c \quad (7a)$$

$$T(r, \frac{l}{2}) = T_h \quad (7b)$$

$$-k[\partial T(a, z)/\partial r] = h [T(a, z) - T_a] \quad (7c)$$

where $h = 4 \sigma \varepsilon \bar{T}^3$, r is the radial coordinate and z the longitudinal coordinate. The assumptions Eqs. (7a) and (7b) are particularly well suited to the problem, in that the ends of the specimen are covered with a thin layer of solder. Applying the boundary conditions Eq. (7) to the solution of Eq. (6) in cylindrical coordinates,

$$\partial^2 T/\partial r^2 + (1/r)(\partial T/\partial r) + \partial^2 T/\partial z^2 = -J^2 \rho / k \quad (8)$$

We obtain⁽⁵⁾

$$\begin{aligned} T(r, z) - T_a &= \sum_{n=0}^{\infty} \frac{2\Gamma}{(\lambda_n a)^2 + \Gamma^{2/l}} \left[\frac{T_h - T_c}{2} \frac{\sinh \lambda_n z}{\sinh \lambda_n l/2} \right. \\ &+ \left(\bar{T} - T_a - \frac{J^2 \rho a}{k \lambda_n^2} \right) \frac{\cosh \lambda_n z}{\cosh \lambda_n l/2} \left. \right] \\ &\frac{J_0(\lambda_n r)}{J_0(\lambda_n a)} \\ &+ \frac{J^2 \rho a}{2h} \left[\frac{\Gamma}{2} \left(1 - \frac{\Gamma^2}{a^2} \right) + 1 \right] \quad (9) \end{aligned}$$

where $\Gamma = ha/k$ and λ_n is a solution of

$$(\lambda_n a) J_1(\lambda_n a) = \Gamma J_0(\lambda_n a) \quad (10)$$

2) Energy Balance at the Thermoelectric Materials Junctions⁽⁵⁾

The total energy which is delivered to the sample at $z = -\frac{l}{2}$, W is evidently the sum of two terms

$$W = 2\pi \int_0^a U_z(r, -\frac{l}{2}) r dr + \pi a^2 h (T_c - T_a) \quad (11)$$

where

U_z is the z component of the energy flux, Eq. (2). The first term in Eq. (11) is due to the energy current entering the sample, and the second is due to the radiation from the face of the sample. The area of the lead wire is ignored compared to the area of the sample.

From Eqs. (2), (9)

$$\begin{aligned}
 U_z(r, -\frac{l}{2}) &= (\alpha T_c + A)J - k \frac{\partial T(r, -\frac{l}{2})}{\partial z} \\
 &= (\alpha T_c + A)J - \sum_{n=0}^{\infty} \frac{2k \lambda_n \Gamma}{(\lambda_n a)^2 + \Gamma} \\
 & \quad \left[\frac{T_h - T_a}{2} \coth \frac{\lambda_n l}{2} \right. \\
 & \quad \left. - (\bar{T} - T_a - \frac{J^2 \rho}{k \lambda_n^2}) \tanh \frac{\lambda_n l}{2} \right] - \frac{J(\lambda_n r)}{J(\lambda_n a)} \quad (12)
 \end{aligned}$$

Thus, from Eqs. (11) and (12)

$$\begin{aligned}
 W &= (\alpha T_c + A)I - \sum_{n=0}^{\infty} \frac{4\pi k \Gamma^2}{\lambda_n [(\lambda_n a)^2 + \Gamma^2]} \\
 & \quad \left[\frac{T_h - T_a}{2} \coth \frac{\lambda_n l}{2} \right. \\
 & \quad \left. - (\bar{T} - T_a - \frac{J^2 \rho}{k \lambda_n^2}) \tanh \frac{\lambda_n l}{2} \right] \quad (13) \\
 & \quad + \pi a^2 h(T_c - T_a)
 \end{aligned}$$

Similarly, at $z = \frac{l}{2}$

$$\begin{aligned}
 W &= (\alpha T_h + A)I - \sum_{n=0}^{\infty} \frac{4\pi k \Gamma^2}{\lambda_n [(\lambda_n a)^2 + \Gamma^2]} \\
 & \quad \left[\frac{T_h - T_c}{2} \coth \frac{\lambda_n l}{2} \right. \\
 & \quad \left. - (\bar{T} - T_a - \frac{J^2 \rho}{k \lambda_n^2}) \tanh \frac{\lambda_n l}{2} \right] \quad (14) \\
 & \quad - \pi a^2 h(T_h - T_a)
 \end{aligned}$$

From theoretical analysis, the thermal conductivity of the sample can be determined from measurements of the current, hot and cold junction temperature, geometry and emissivity of the sample. The factor involving contact resistance is eliminated experimentally by carrying out measurements for both directions of current. The current, hot and cold junction temperatures, and sample dimensions are easily measurable parameters.

3. PREPARATION OF THERMOELECTRIC DEVICES

The initial step in the growth of high quality films is the preparation of the substrate prior to insertion into the chamber. The substrates were

first cleaned with ammonia hydrogen peroxide-ammonia-HCl. And the contamination layer of substrates was removed by etching in a 50% HF solution, rinsed in a cascade rinse for 10min., then spun dry.

After the substrate is properly cleaned and etched it may be introduced into the ICBE⁽⁶⁾(Ionized Cluster Beam Epitaxy) system to growth thin film for thermoelectric device.

The ICBE system specifically constructed for the present study is shown in Fig. 2. Four separate crucibles for Bi, Sb, Te and Se are used to independently control the temperature of the source material in each crucible. In this respect, ICBE similar to MBE. The similarity between ICBE and MBE, however, stops here since in ICBE the crucible is covered with a cap having a small flow-constricting nozzle which allows one to maintain a much higher vapor pressure inside the crucible than that of MBE. It is because of this nozzle that the vapor coming out of the crucible adiabatically expands into a vacuum resulting in small aggregates of atoms, namely, "clusters". Once produced, these clusters are impact ionized using thermionic electrons, accelerated in an electric field, and delivered to a heated substrate for material deposition. The ratio of ionized to neutral clusters in the ionized cluster beam, the energy with which the ionized clusters impinge upon the substrate, the size of clusters, and the substrate temperature then become the parameters controlling the morphology, smoothness, and other properties of the growing film.

The ICBE system schematically illustrated by Fig. 2 is housed in a vacuum bell jar whose base pressure was typically 5×10^{-9} Torr for all the thin-film growth runs. A typical experimental sequence for the growth of thin film is as follows. First turn on the crucible and heat the substrate to the desired temperature. Then turn on the ionizer and supply an accelerating field to the ionized As beam so that, when the energetic beam hits the substrate, it can remove the native contamination layer. The energy of the As beam

and the time duration over which it is directed onto the substrate therefore control the substrate cleaning. While cleaning is being done start heating the crucibles of source materials. The next step is to start the film growth process by opening the shutter to the crucibles of source materials.

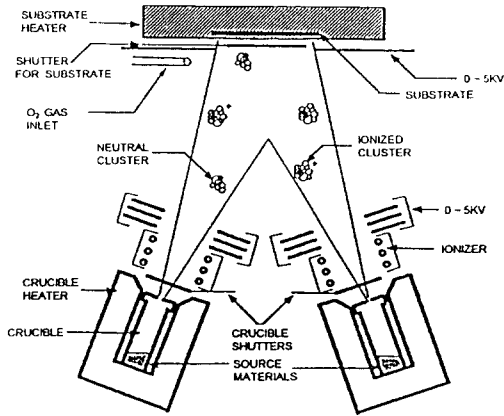


Fig. 2 Schematic of ICBE system

After the thin films grown on the substrate using these procedures are analyzed by a SEM picture, a TEM analysis and a XRD pattern.

After this step, a solderable ceramic insulated thermoelectric module. Each module contains several thermoelectric device elements, each element with 0.25cm in length and 5.0mm² in cross section. Thermoelectric material is a quaternary alloy of bismuth, tellurium, selenium, and antimony with small amounts of suitable dopants(Cu, Si, Fe, Mg), carefully processed to produce an oriented polycrystalline ingot with superior anisotropic thermoelectric properties. Metallized ceramic plates afford maximum electrical insulation and thermal conduction.

Procedure for the preparation of samples as follows.

1. Prepare cold plate and heat sink surfaces.
2. Thoroughly clean and degrease thermoelectric module heat sink and cold surface.
3. Apply a thin continuous film of thermal grease to module hot side surface and to module area on heat sink.
4. Locate module on heat sink, hot side down.

5. Gently oscillate module back and forth, exerting uniform downward pressure, noting efflux of thermal compound around edges of module.
6. Repeat step 3 for cold side surface and cold plate.
7. Position cold plate on module.
8. Repeat step 5, sliding cold plate instead of module.
9. Before bolting, best results obtained by preloading in compression the cold plate/heat sink/module assembly, applying light load in line with center of module using clamp or weights. For two modules assemblies, use 3 screws located on module center line, with middle screw located between modules.
10. Lead wires are soldered to module tabs with bismuth/tin solder.

The cross sections of the experimental fabricated thermoelectric devices in this paper are shown Fig. 3 with design parameters. Tabel 1 gives the design parameters and the process parameters in thermoelectric devices

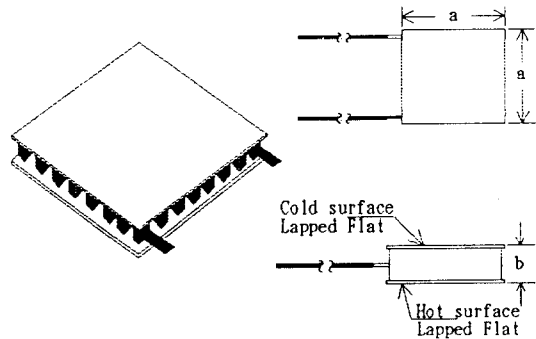


Fig. 3 The structure of thermoelectric device

Table 1. Design and process parameters in thermoelectric devices

Parameters	a(cm)	b(cm)
Samples		
KU-1	5.44	0.51
KU-2	2.97	0.56
KU-3	3.96	0.46
KU-4	5.44	0.58

4. EXPERIMENTAL RESULTS

Peltier cooling and heating was determined by means of two thermoelectric materials junctions placed approximately. To evaluate the performance of thermoelectric devices, measurements of $T_h - T_c$ characteristics and the $I - \Delta T$ characteristics were performed.

Fig. 4 ~ Fig. 7 show plots of the cooling and heating characteristics of thermoelectric devices as a function of current for different heat sink temperature (T_h).

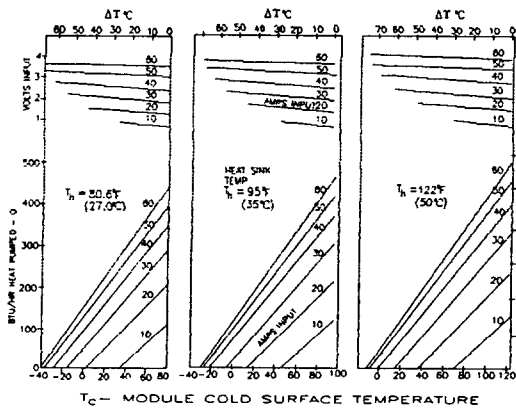


Fig. 4 The characteristics of cooling and heating in thermoelectric device (sample KU-1)

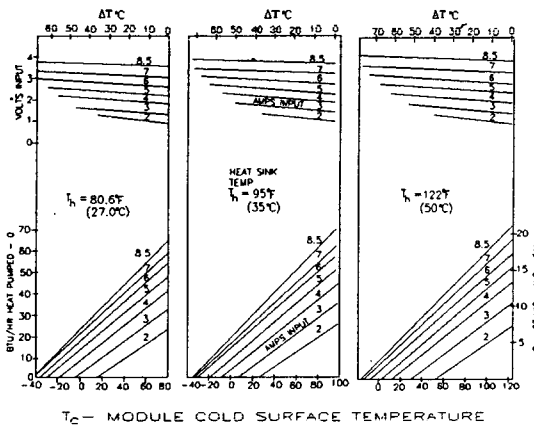


Fig. 5 The characteristics of cooling and heating in thermoelectric device (sample KU-2)

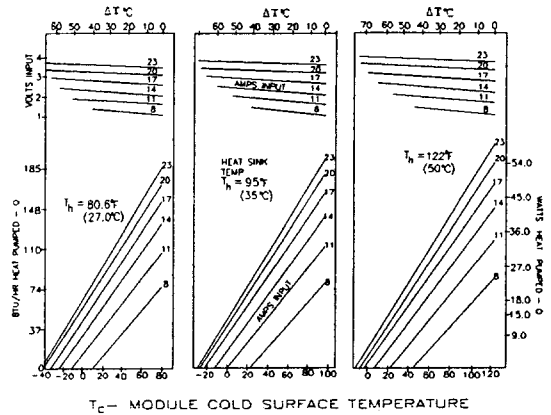


Fig. 6 The characteristics of cooling and heating in thermoelectric device (sample KU-3)

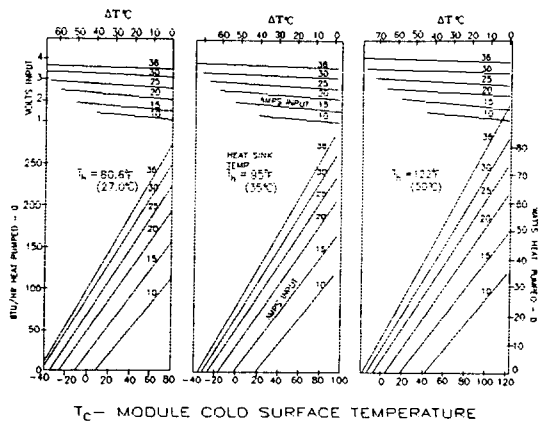


Fig. 7 The characteristics of cooling and heating in thermoelectric device (sample KU-4)

5. DISCUSSIONS

The optimum thermoelectric materials are extrinsic compound semiconductors with carrier concentrations in the range 10^{19} electrons(or holes) per cm^3 . To maximize the performance of thermoelectric devices, one part is made of p-type material and the other part of n-type material.⁽⁷⁾⁽⁸⁾ The junction between the two parts thus assumes the character of a p-n junction and is shown schematically in Fig. 8. To the left of the junction, the current carried primarily

by holes, whereas to the right it is carried primarily by electrons. For the direction of current shown, hole-electron pairs must be thermally created, and the junction is a heat-absorbing junction. The thermal energy required to make a hole-electron pair is just the vertical projection of the transition arrow shown in Fig. 8, and this is seen to be in accord with the usual definition of Peltier coefficient

$$\pi_{12} = T(S_2 - S_1) \quad (15)$$

where $S = (\frac{1}{e})(Bk - A/T)$. S is the Seebeck coefficient, T is the absolute temperature of junction, k is Boltzmann's constant, and A is electrochemical potentials. B is a number which depends upon the precise mechanism of charge carrier scattering ($B=2$ for scattering by acoustical phonons). The quantity BkT may be regarded as the average thermal energy of charge carriers emitted from junction.⁽⁹⁾⁽¹⁰⁾

Electron-hole pairs are created by vertical transitions across the full energy gap after which the created carriers diffuse and drift in the isothermal junction region. The net thermal energy absorbed per pair is the same as indicated, but the transport of charge through the junction is impeded by the rectifying contact. The situation is improved by replacing the junction with a metal weld as shown in Fig. 9, but a single metal cannot in general eliminate the rectifying contacts at both surfaces.

In Fig. 10 we show the establishment of ohmic contacts at both surfaces by using a low work function metal in contact with the n-type material and a high work function metal in contact with the p-type material. The importance of an ohmic contact for many semiconductor applications is well known, but its importance for high current Peltier junction has apparently not received adequate discussion. At appreciable current levels a rectifying contact is accompanied by voltage drop across the contact; this may be interpreted in terms of a contact resistance, but actually it is a reduction in Peltier coefficient of the heat absorbing

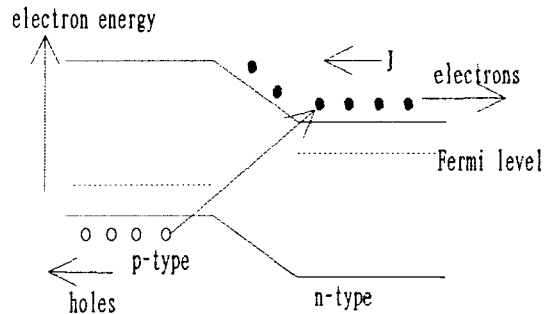


Fig. 8 An isothermal junction between p-type and n-type semiconductor at low current density. This is a heat absorbing junction for direction of current shown.

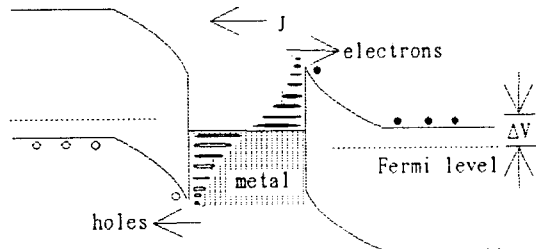


Fig. 9. An isothermal semiconductor-metal-semiconductor junction at high current density

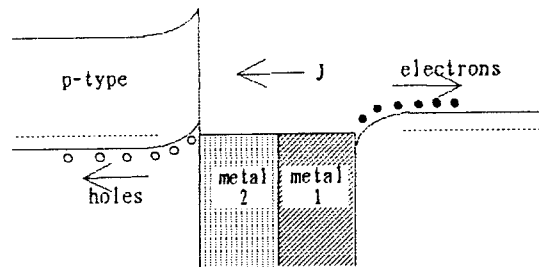


Fig. 10. An ohmic junction at low or high current density. Metal 1 has a low work function and metal 2 has a high work function

junction and an increase in Peltier coefficient of the heat producing junction.

This statement follows from an examination of Fig. 9 where, as usual, the voltage drop across the junction (ΔV) is depicted as a shift in Fermi level. The net thermal energy to create

an electron-hole pair is thus reduced by an amount $e\Delta V$. Note that at the heat absorbing junction, current flows through the rectifier in the reverse direction, but at the heat producing junction its passage is in the forward direction.

Thus the presence of a rectifying contact reduces the efficiency of the thermoelectric devices as the current density is increased. Since current densities in power generating thermoelectric devices may run as high as several hundred amperes/cm², the effect appears to be important.

The rectifying contact can probably not be eliminated completely in practical thermoelectric devices. The choice of semiconductor for a thermoelectric application is controlled by its figure of merit, and the choice of junction metal is limited by considerations of chemical compatibility and stability.

These best materials which have been available for thermoelectric cooling devices are alloys of bismuth telluride with bismuth selenide and antimony telluride. Therefore in our experiments, we have fabricated the thermoelectric devices with (BiSb)₂Te₃ and Bi₂(TeSe)₃ to obtain the best thermoelectric characteristics.

6. CONCLUSIONS

This paper has presented the characteristics of thermoelectric devices and the plots of thermoelectric cooling and heating as a function of currents for different temperatures. The maximum cooling and heating (ΔT) for (BiSb)₂Te₃ and Bi₂(TeSe)₃ as a function of currents is about 75°C.

A solderable ceramic insulated thermoelectric module. Each module contains 31 thermoelectric devices. Thermoelectric material is a quaternary alloy of bismuth, tellurium, selenium, and antimony with small amounts of suitable dopants, carefully processed to produce an oriented polycrystalline ingot with superior anisotropic thermoelectric properties. Metallized ceramic plates afford maximum electrical insulation and thermal conduction. Operating

temperature range is from -156°C to +104°C. The amount of Peltier cooling is directly proportional to the current through the sample, and the temperature gradient at the thermoelectric materials junctions will depend on the system geometry.

7. ACKNOWLEDGEMENT

The authors are grateful to EESRI(Seoul National University) for the interest in this work and continual encouragement. This work was supported by the KEPCO through Grant No. 94-019

REFERENCE

- (1) M. Idnurm and K. Landecker, "Experiments with Peltier Junctions Pulsed with High Transient Currents", J. Appl. Phys., Vol. 34, No. 6, 1963
- (2) E. K. Stefanakos, A. Abul-Fadl, and M. D. Workman, "Measurements of Peltier Cooling at a Ga-GaAs Interface Using a Liquid Phase Epitaxy System", J. Appl. Phys., Vol. 46, No. 7, 1975
- (3) S. Hava, H. B. Sequeira, and R. G. Hunsperger, "Thermoelectric and Thermal Properties of GaAlAs Peltier-Cooled laser Diodes", J. Appl. Phys., Vol. 58, No. 5, 1985
- (4) G. E. Smith and R. Wolfe, "Thermoelectric Properties of Bismuth-Antimony Alloys", J. Appl. Phys., Vol. 33, No. 3, 1962
- (5) S. Vojdani, A. E. Dabiri and M. Tavakoli, "The Oretical Aspects of the Peltier Effect on the Temperature Distribution in Crystal Grown by the Czochralski Technique", J. Electrochem. Soc. : Solid State Sci. & Tech., Vol. 122, No. 10, 1975
- (6) Man Y. Sung, "A Study on the Electrical Characteristics and the Growth of Al₂O₃ Film on Si with Low Temperatures by GAIVBE System", Research Report, ISRC 94-E-1015
- (7) Abul-Fadl and E. K. Stefanakos, "Peltier Cooling at a In-InP Interface", J. Appl. Phys., Vol. 47, No. 10, 1976

- (8) Milivoj Belic, "A Solid State Solar Powered Heat Transfer Device", J. Appl. Phys., Vol. 50, No. 9, 1979
- (9) Gunther Rotzer, Loren Lockwood, and Jose L. Gilz, "Measurement of Thermoelectric Coefficients at the Solid Liquid Interface of Highly Doped P-type Silicon", J. Appl. Phys., Vol. 48, No. 2, 1977
- (10) Jeffrey M. Belling and Joe Unsworth, "Modified Angstrom's Method for Measurement of Thermal Diffusivity of Materials with Low Conductivity", Rev. Sci. Instrum., Vol. 58, No. 6, 1987
- (11) T. Nakano and T. Hashimoto, "Refrigeration Character of New-Type Peltier Refrigerator Using High T_c (Bi, Pb)₂Sr₂Ca₂Cu₃O_x Superconductor", Jpn. J. Appl. Phys. Part 2-Letters, Vol. 33, pp. L1728~L1731, 1994
- (12) M. Galfy, C. Hohn, A. Freimuth, "Peltier-Effect in the mixed-state of (Bi, Pb)₂Sr₂Ca₂Cu₃O-Delta", Annalen der Physik, Vol. 3, pp. 215~224, 1994
- (13) P. Wilding, M. A. Shoffner, L. J. Kricka, "PCR in a Silicon Microstructure", Clinical Chemistry, Vol. 40, pp. 1815~1818, 1994

저자소개



성만영

1949년 6월 3일생. 1974년 고려대학교 전기공학과 졸업. 1981년 동 대학원 졸업(공학). 1985년 Univ. of Illinois 부교수. 현재 고려대학교 전기공학과 교수.



송대식

1970년 6월 21일생. 1994년 8월 고려대학교 공대 전기공학과 졸업. 현재 동 대학원 석사과정.



배원일

1971년 4월 27일생. 1994년 2월 고려대학교 공대 전기공학과 졸업. 현재 동 대학원 석사과정.